



This is a repository copy of *Integrating the physics with data analytics for the hybrid modeling of the granulation process*.

White Rose Research Online URL for this paper:
<http://eprints.whiterose.ac.uk/119654/>

Version: Accepted Version

Article:

AlAlaween, W.H., Mahfouf, M. and Salman, A.D. (2017) Integrating the physics with data analytics for the hybrid modeling of the granulation process. *AIChE Journal*. ISSN 0001-1541

<https://doi.org/10.1002/aic.15831>

Reuse

Items deposited in White Rose Research Online are protected by copyright, with all rights reserved unless indicated otherwise. They may be downloaded and/or printed for private study, or other acts as permitted by national copyright laws. The publisher or other rights holders may allow further reproduction and re-use of the full text version. This is indicated by the licence information on the White Rose Research Online record for the item.

Takedown

If you consider content in White Rose Research Online to be in breach of UK law, please notify us by emailing eprints@whiterose.ac.uk including the URL of the record and the reason for the withdrawal request.



eprints@whiterose.ac.uk
<https://eprints.whiterose.ac.uk/>

Integrating the Physics with Data Analytics for the Hybrid Modelling of the Granulation Process

Wafa' H. AlAlaween^a, Mahdi Mahfouf^a and Agba D. Salman^b

^aDepartment of Automatic Control and Systems Engineering, The University of Sheffield, UK

^bDepartment of Chemical and Biological Engineering, The University of Sheffield, UK

(E-mails: whalalaween1@sheffield.ac.uk; m.mahfouf@sheffield.ac.uk;
a.d.salman@sheffield.ac.uk)

Abstract

In this paper, a hybrid model based on physical and data interpretations to investigate the high shear granulation (HSG) process is proposed. This model integrates three separate component models, namely, a computational fluid dynamics model, a population balance model and a radial basis function model, through an iterative procedure. The proposed hybrid model is shown to provide the required understanding of the HSG process, and to also accurately predict the properties of the granules. Furthermore, a new fusion model based on integrating fuzzy logic theory and the Dempster-Shafer theory is also developed. The motivation for such a new modelling framework stems from the fact that integrating predictions from models which are elicited using different paradigms can lead to a more robust and accurate topology. As a result, significant improvements in prediction performance have been achieved by applying the proposed framework when compared to single models.

Keywords: Hybrid model; Data fusion; Fuzzy logic; Dempster-Shafer theory; High shear granulation.

Introduction

In the pharmaceutical, chemical, food, agricultural and many other industries, granulation is a key unit operation of the manufacturing cycle and the development of the final product¹.

In particular, high shear granulation (HSG) has been extensively used because of its short processing time due to the fast growth and densification processes². In general, granulation is recognised as being a complex process with three distinct mechanisms taking place all inside the granulator itself, namely: 1. Wetting & nucleation, 2. Growth & consolidation, and 3. Breakage & attrition³. Despite the huge body of research addressing the different issues of the granulation process, it remains a subject of active research. The reason behind this can be attributed to the inherent complexity of such a process which results in the poor understanding of the process and its mechanisms and, consequently, leading to a high recycling ratio and significant wastes in the related industries⁴. Consequently, recent studies have focused on the understanding, the modelling and the simulating of the granulation process. The various modelling paradigms that have been developed and applied are either data-driven (e.g. neural network) or physical based models (e.g. population balance model)^{1, 5-7}.

Data-driven models have been mainly utilized to predict the properties of the granules using different granulation equipment and materials⁸. There are however some significant advantages of using these paradigms. The number of properties to be monitored can be large compared to physical based models, where studying more than three properties can be computationally taxing. Furthermore, these models map the granulation inputs to the outputs without the need for representation of the complex nature of the process and the interactions among its mechanisms. Thus, they can successfully predict the properties of the granules and can simply interpret the relationships between the inputs and the outputs in a way that one can easily understand and relate to¹.

Physical based models have also been utilized to gain a deeper insight into the physics behind the granulation process. In particular, population balance models (PBMs) have received a great deal of interest when it comes to modelling such a process⁵. One dimensional PBM was more commonly used, where the size of the granules was investigated, assuming that the size

has the main effect and it may affect other properties⁹. However, the consideration of the binder content and the porosity of the granules is crucial. Likewise, the one dimensional model is unable to capture the complex interactions among the granulation mechanisms⁹. These limitations reinforce the need to develop a multi-dimensional model. Three-dimensional models have been employed to predict the main properties of the granules, whereas the three granulation mechanisms have been represented by developing various kernels, which are either empirically or semi-mechanistically derived⁵. Modelling the granulation process using the PBMs has hitherto provided a good understanding of the process at the micro-level¹⁰. These models depend mainly on the impact velocity which is a function of the granule position from the impeller. They also depend on the overall flow pattern of the granules inside the mixer. However, such parameters cannot be extracted from these models. Moreover, one of the main difficulties that has been addressed is the representation of the interactions among the mechanisms which play a crucial role in shaping the properties of the granules¹. Thus, various stochastic and mechanistic models have been utilized to provide the necessary understanding of the flow pattern and the impact velocity of the granules¹¹⁻¹². The discrete element method (DEM), as a stochastic approach, tracks every single particle in the mixer. In practice, such a method may however be computationally taxing since more than a billion particles have to be considered, which is the case for the HSG mixer¹². Recently, a computational fluid dynamics (CFD) model has been utilized to model a multiphase flow¹¹. In particular, the so-called Eulerian multiphase model has been widely employed to simulate flow with both dispersed and continuous phases, and also to take account of the interactions between these phases¹³. In this model, the mean diameter is used to represent the size distribution of the dispersed phase. Such an assumption may lead to inaccurate modelling results when the size distribution is multimodal or wide. Therefore, incorporating the CFD model with the PBM would circumvent the limitations of employing each model separately¹¹.

In the granulation process, the successful model is one that (i) can accurately predict the properties of the granules, (ii) can provide the required understanding of the process and its mechanisms, and (iii) can be used reliably and efficiently by the relevant industries. In fact, all of the above objectives may not be achievable by using one single model. Therefore, in this research, a hybrid model integrating both data and physical based models is developed. Such a model integrates three separate but synergetic models through an iterative procedure. The hybrid model consists of three models, namely; a CFD model, the three-dimensional PBM and a radial basis function (RBF) model. These models are integrated in such a way that the outputs from one of these models are used as inputs to the other model. In order to improve the modelling performance of the hybrid model, a new fusion model based on fuzzy logic theory and the Dempster-Shafer theory is also proposed. The main idea behind this model is to combine the predicted outputs from different models to obtain more accurate predictions, which may not be obtainable using a single model. Thus, the predicted outputs from the hybrid model are combined with the ones from the model incorporating the integrated network and the Gaussian mixture model. This model, which will be from now on referred to as the incorporated model, is a data-driven model that was previously developed to predict the properties of the granules produced by the same equipment and materials, which were used in this research¹, the integrated network is described in Appendix. The remainder of the paper is organized as follows: first, the experimental work that was conducted using the Eirich high shear mixer is described. The hybrid model and the related theoretical background are then presented, the results are also presented and discussed, followed by presenting the new fusion approach and its results. Finally, concluding remarks summarise the work with recommendations for future research.

Experimental Work

The high shear Eirich mixer (1 Litre vertical axis granulator with a top-driven impeller, Maschinenfabrik Gustav Eirich GmbH & Co KG, Germany) was used to granulate Calcium Carbonate ($D_{50}=85\mu\text{m}$) by adding Polyethylene Glycol (PEG 1000). This mixer is equipped with a scraper and impellers with different shapes. It is worth mentioning at this stage that only two impellers were used in this research, as shown in Figure 1; the two impellers not being in the centre of the 16cm diameter vessel. Before the start of the granulation experiment, the binder was melted (the melting point is approximately 40°C), followed by pouring-in the binder on the powder bed while both the vessel and the impeller were rotating in the same direction (clockwise). For all experiments, the binder addition lasted for approximately three minutes. Once the granulation experiment was completed, the granules were left at room-temperature to allow the binder to solidify. Finally, these granules were characterized in terms of size, which was measured using the Retsch camsizer (Retsch Technology GmbH, Germany), binder content and porosity, which were measured in the size range ($180\text{-}2000\mu\text{m}$) as described in¹.

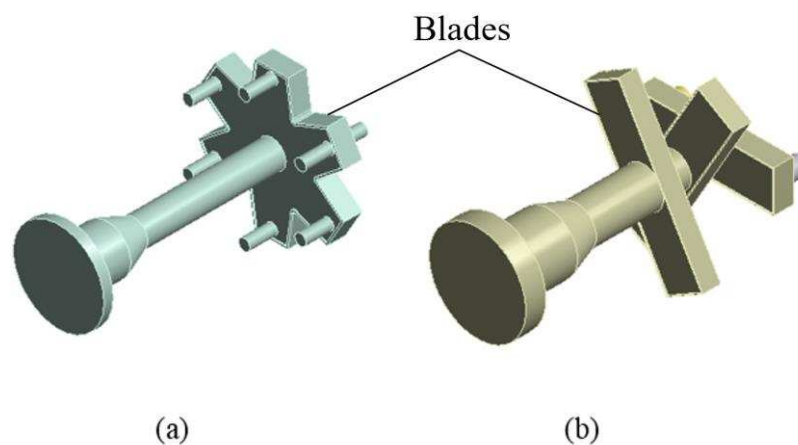


Figure 1. CAD drawing of the impeller types (a) impeller type I, bin impeller, and (b) impeller type II, star impeller (Reproduced with Permission from Maschinenfabrik Gustav Eirich GmbH & Co KG., January 2017).

Four input variables were investigated, namely, impeller speed (from 1000 to 6000 rpm), granulation time (6, 10 and 15 minutes), L/S ratio (13, 14 and 15%) and impeller shape (two

impeller shapes were used). The granulation vessel was at the horizontal position during the granulation process (i.e. tilt angle was zero) and its speed was kept constant (170rpm). Generally, many input variables can affect the granulation process, however, the specifically investigated variables proved to have the most significant effects, which were measured via the correlation coefficient, in terms of the final properties of the granules produced using Calcium Carbonate. The aforementioned variables were systematically studied using a full factorial design of experiments; the total number of experiments being 108.

The Hybrid Model

The Hybrid Model: Model Development

Granulation is a complex process due to the different interactive mechanisms occurring inside the granulator. Such a process is also influenced by many controllable and uncontrollable factors which may possibly have conflicting effects. In addition to the ones mentioned in¹, these are some of the serious difficulties that may limit the performance of a single model. In this research, a hybrid model consisting of both data and physical based models has been developed. Figure 2 illustrates the simple iterative scheme of the hybrid model. Based on the granulation input variables and the mixer geometry, a CFD model is developed to analyse the overall flow pattern of the granules, their distribution and the velocity inside the mixer. The output parameters from this model (e.g. impact velocity) are crucial to predict the main properties of the granules using a PBM such as the granule size. It is well-known that some empirical parameters are required to implement the PBM⁶. Therefore, a radial basis function (RBF) model is included to estimate these parameters by mapping them directly to the granulation input variables. Such a model can implicitly compensate for the assumptions that have been made to simplify the computational efforts required by the physical models, for instance, the homogeneous mixing features of the overall flow of the granules. In addition, this

model is used to express these parameters as a function of the input variables, therefore, a better knowledge relating the effects of the input variables on these parameters and on the final properties of the granules is gained. The size of the granules predicted by the PBM is then used to re-evaluate the parameters obtained from the CFD model, followed by re-estimating the outputs of the PBM and RBF model. The steps above are repeated until a satisfactory performance is reached, or alternatively the difference between the predictions for two consecutive steps becomes asymptotically small. It is worth emphasising at this stage that the performance of the hybrid model depends on the performances of the models included.

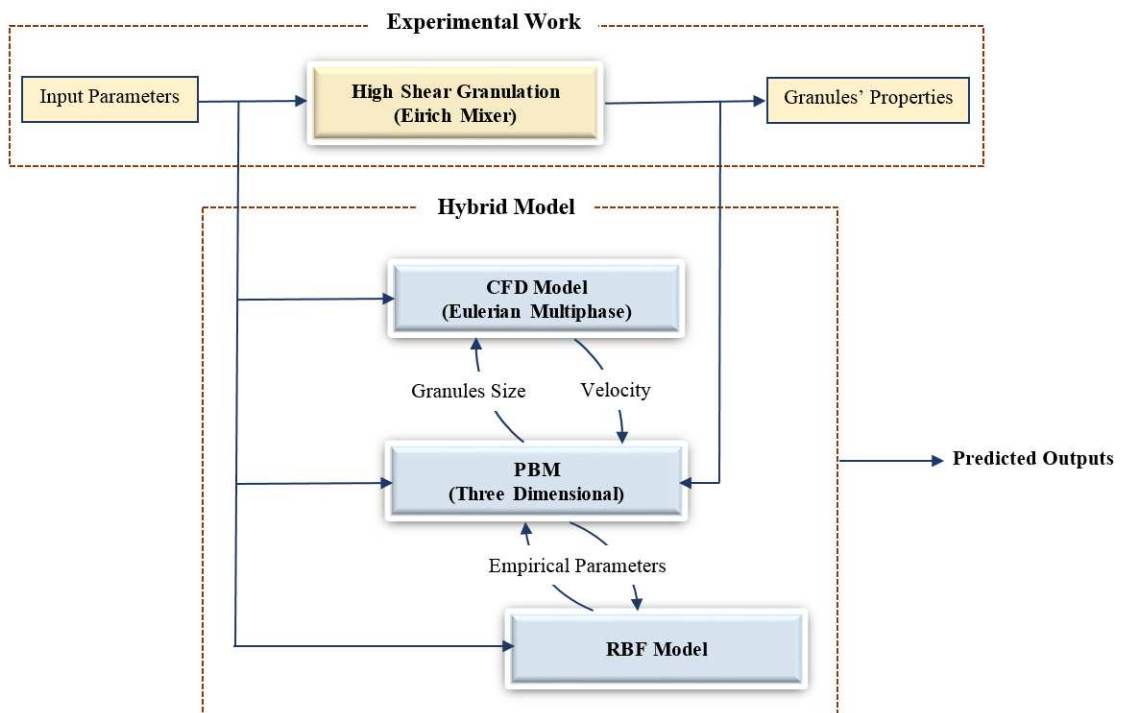


Figure 2. The hybrid model for the HSG process.

The mathematics behind the single models presented have already been well-publicised. Readers may refer to various research papers and books for further readings, in particular references^{3-7, 9-25}. In this paper, only the key developments are included in order to help the reader get to grips with the algorithms presented.

Population Balance Model

As already stated, a three-dimensional PBM provides a deeper insight into the granulation process by representing its three main mechanisms. This is because it follows the evolution of the granules with time by virtue of the granule size, the binder content and the porosity. The 3D population balance equation is usually written as follows¹⁴:

$$\frac{\partial}{\partial t} F(s, l, g, t) + \frac{\partial}{\partial s} \left(F(s, l, g, t) \frac{ds}{dt} \right) + \frac{\partial}{\partial l} \left(F(s, l, g, t) \frac{dl}{dt} \right) + \frac{\partial}{\partial g} \left(F(s, l, g, t) \frac{dg}{dt} \right) = \mathfrak{R}_{\text{Nucleation}} + \mathfrak{R}_{\text{Aggregation}} + \mathfrak{R}_{\text{Breakage}} \quad (1)$$

where $F(s, l, g, t)$ represents the density function such that $F(s, l, g, t) ds dl dg$ is the mass of granules when solid (s), liquid (l) and gas (g) are in the ranges $(s, s+ds)$, $(l, l+dl)$ and $(g, g+dg)$, respectively. The partial derivatives with respect to s , l and g account for layering, drying and re-wetting, and consolidation, respectively. The terms in the right hand-side of (1) stand for the rates of nucleation, aggregation and breakage. Various nucleation rates have been developed, however, the majority of these assumes that one droplet forms a nucleus. However, the latter assumption is not always valid¹⁰. Since the breakage of nuclei plays a significant role in the nucleation mechanism¹⁵, an empirical nucleation rate was used in this study. The aggregation rate consists of two terms, formation and depletion, which can be written as follows¹⁰:

$$\begin{aligned} \mathfrak{R}_{\text{Aggregation}} &= \mathfrak{R}_{\text{Aggregation}}^{\text{Formation}} + \mathfrak{R}_{\text{Aggregation}}^{\text{Depletion}} \\ \mathfrak{R}_{\text{Aggregation}}^{\text{Formation}} &= \frac{1}{2} \int_{s'=s_{\text{nuc}}}^{s-s_{\text{nuc}}} \int_{l'=0}^l \int_{g'=0}^g \beta(s', s-s', l', l-l', g', g-g') \times F(s', l', g', t) \\ &\quad \times F(s-s', l-l', g-g', t) ds' dl' dg' \\ \mathfrak{R}_{\text{Aggregation}}^{\text{Depletion}} &= F(s, l, g, t) \int_{s'=s_{\text{nuc}}}^{s-s_{\text{nuc}}} \int_{l'=0}^l \int_{g'=0}^g \beta(s', s, l', l, g', g) \\ &\quad \times F(s', l', g', t) ds' dl' dg' \end{aligned} \quad (2)$$

where s_{nuc} is the volume of the nucleus, and $\beta(s', s-s', l', l-l', g', g-g')$ is the aggregation kernel which governs the rate at which two granules with internal coordinates (s', l', g') and $(s-s', l-l', g-g')$ agglomerate. In fact, the coalescence of two granules depends on the

granules size and the availability of the binder on their surfaces. The semi-mechanistic aggregation kernel that describes these two factors and the coalescence types has been already presented in¹⁶. Such a kernel can be expressed as follows¹⁶:

$$\beta = \zeta \frac{4\pi u_0 (R_1 + R_2)^2}{W} \quad (3)$$

$$W = \left\{ \begin{array}{l} (R_1 + R_2) \int_{R=R_1+R_2}^{\infty} \frac{\exp\left(\frac{\psi}{kT}\right)}{R^2} dR, \quad \text{Type I coalescence} \\ (R_1 + R_2) \left(\max \left(\int_{R=R_1+R_2}^{\infty} \frac{\exp\left(\frac{-\psi_{\text{forward}}}{kT}\right)}{R^2} dR, \int_{R=R_1+R_2}^{\infty} \frac{\exp\left(\frac{-\psi_{\text{reverse}}}{kT}\right)}{R^2} dR \right) \right), \quad \text{Type II coalescence} \end{array} \right.$$

where R_i is the radius of the i^{th} particle, u_0 and W are the initial velocity of the particle and the Fuch stability ratio, respectively. The parameters k and T represent the Boltzmann constant and the temperature, respectively. The parameter ψ refers to the net attractive potential for coalescence, and ζ is a tuneable parameter.

The consolidation mechanism takes account of the compaction process that increases the binder on the surface of granules and leads to a decrease in the porosity. The consolidation process has been empirically expressed by the following set of equations:

$$\varepsilon = \frac{1 + g}{s + 1 + g} \quad (4)$$

$$\frac{d\varepsilon}{dt} = -c(\varepsilon - \varepsilon_{\min})$$

$$\frac{dg}{dt} = -c \frac{s + 1 + g}{s(1 - \varepsilon_{\min})} \left(1 - \frac{\varepsilon_{\min} s}{1 - \varepsilon_{\min}} + g \right)$$

where ε and ε_{\min} are the porosity and its minimum value, respectively. The constant c is the compaction rate constant. The breakage rate was stochastically estimated based on the algorithm developed in¹⁷. Such an algorithm is based on determining the likelihood that a granule in a specific size class breaks to form a number of granules in smaller size classes.

Computational Fluid Dynamics

Generally, numerical simulation techniques of a system can be classified into two types; continuum and discrete. As the names indicate, the former views the system as a continuous flow (i.e. fluid), while the latter deals with an individual particle. An Eulerian multiphase model is used to simulate the particulate phase as a continuous flow¹⁸. Two phases; solid and gas, are considered. The mass and momentum of these two phases are governed by the following set of equations¹⁹:

$$\begin{aligned}
 \frac{\partial(\alpha_g \rho_g \mathbf{u}_g)}{\partial t} + \nabla \cdot (\alpha_g \rho_g \mathbf{u}_g \mathbf{u}_g) &= -\alpha_g \nabla P + \nabla \cdot (\alpha_g \boldsymbol{\tau}_g) - \gamma(\mathbf{u}_g - \mathbf{u}_s) + \mathbf{F} \\
 \frac{\partial(\alpha_g \rho_g)}{\partial t} + \nabla \cdot (\alpha_g \rho_g \mathbf{u}_g) &= 0 \\
 \frac{\partial(\alpha_s \rho_s \mathbf{u}_s)}{\partial t} + \nabla \cdot (\alpha_s \rho_s \mathbf{u}_s \mathbf{u}_s) &= -\alpha_s \nabla P + \nabla P_s + \nabla \cdot (\alpha_s \boldsymbol{\tau}_s) - \gamma(\mathbf{u}_g - \mathbf{u}_s) + \mathbf{F} \\
 \frac{\partial(\alpha_s \rho_s)}{\partial t} + \nabla \cdot (\alpha_s \rho_s \mathbf{u}_s) &= 0
 \end{aligned} \tag{5}$$

where α , ρ and \mathbf{u} are the volume fraction, density and velocity, respectively. The subscripts are used to distinguish the parameters of the gas (g) phase from the ones of the solid (s) phase. The volume fractions must sum to unity. The parameters P and F represent the pressure and all the forces acting on the system under investigation, respectively. The interphase momentum exchange coefficient (γ) is calculated using the equation presented in²⁰. The viscous stress tensor ($\boldsymbol{\tau}$) can simply be written as follows¹⁹:

$$\boldsymbol{\tau}_k = \left(\nu_k - \frac{2}{3} \mu_k \right) (\nabla \cdot \mathbf{u}_k) \mathbf{I} + 2\mu_k \mathbf{S}_k \tag{6}$$

where ν and μ represent the bulk and dynamic viscosity of the kth phase, respectively. The parameter S represents the strain rate tensor derived in¹⁹, and I is the second invariant of the strain rate tensor.

By virtue of extension of the kinetic theory of dense gas, one would develop the kinetic theory behind the granular flow (KTGF) model. Such a theory depends on statistical mechanics to describe the velocity of a granular flow. As already outlined in²¹, the KTGF model assumes that particles interaction is binary as well as instantaneous²¹. At a high solid fraction, this may result in high particles/granules stresses. Therefore, the frictional term, or the so-called frictional stress model, should be taken into account when the pressure and the dynamic viscosity of the solid phase are evaluated: the model is further detailed in¹⁹. It is worth mentioning at this stage that, in this study, the angle of internal friction was 44°.

Various boundary conditions have been used in the open literature¹⁹. In this research paper, the ‘no slip’ boundary condition at the vessel, impeller and scraper wall was used for the gas phase. For the solid phase, the ‘partial slip’ model proposed in²² was utilized. The coefficient of restitution was chosen to be 0.5. Such a model is a combination of both ‘no slip’ and ‘free slip’ conditions.

Radial Basis Function Model

RBF model usually maps a set of inputs to an output. RBF network consists of three layers: an input, hidden including basis functions, and an output layer. Such a mapping can be generally given as follows²³:

$$y(\mathbf{x}) = \sum_{i=1}^I w_i \phi_i(\mathbf{x}) + w_0 \quad (7)$$

where w_i and w_0 denote the weights and bias, respectively. \mathbf{x} is the input vector and y is the predicted output which is expressed as a linear combination of the basis functions. RBF is a function of the radial distance from a centre (μ_i). Such function can usually be expressed as follows:

$$\phi_i(\mathbf{x}) = f_i(\|\mathbf{x} - \mu_i\|) \quad (8)$$

where f_i is the basis function. Because of its ability to approximate any function with a reasonable accuracy using a sufficient number of components, the Gaussian form is a popular choice for such a function²³. The predicted outputs in this research are the empirical parameters that are required to implement the PBM. Typically, the available data are divided into training and testing data sets. The training data are used for identifying the relationships between the inputs and the outputs, while the testing data are used to ensure good generalization capabilities measured via the root mean square error (RMSE). The model parameters (e.g. mean) were optimized using the scaled conjugate gradient algorithm²³. The best network structure (i.e. the number of basis functions) is the one that corresponds to the minimum RMSE.

The Hybrid Model: Results and Discussions

To study the flow of the granules inside the granulation vessel, two CFD models were developed using ANSYS software (ANSYS Inc., US, Release 16.1) for simulation of the Eirich mixer with two impellers differing in shape, as shown in Figure 1. Accordingly, two fine-meshing schemes differing in the number of cells were generated. For each model, three different meshing schemes were initially tested, the ones presented in this study are the schemes that led to acceptable solutions. In each model, the gas-solid flow was analysed using a two-fluid model inspired from the KTGF model. The material properties were selected so as to reproduce as closely as possible the properties of air and the properties of the granules produced using 500gm of Calcium Carbonate and different mass values of Polyethylene Glycol. The vessel speed was kept constant during the simulation of all experiments (at 170rpm clockwise), while the values of the impeller speed were assigned corresponding to the operating conditions. The granules were assumed to have initially settled at the bottom of the granulation vessel. A second-order upwind scheme was utilized to solve all the partial differential equations, while the volume fraction equation was solved using a first-order scheme. The model was stopped once it converged, or alternatively a stable flow was observed.

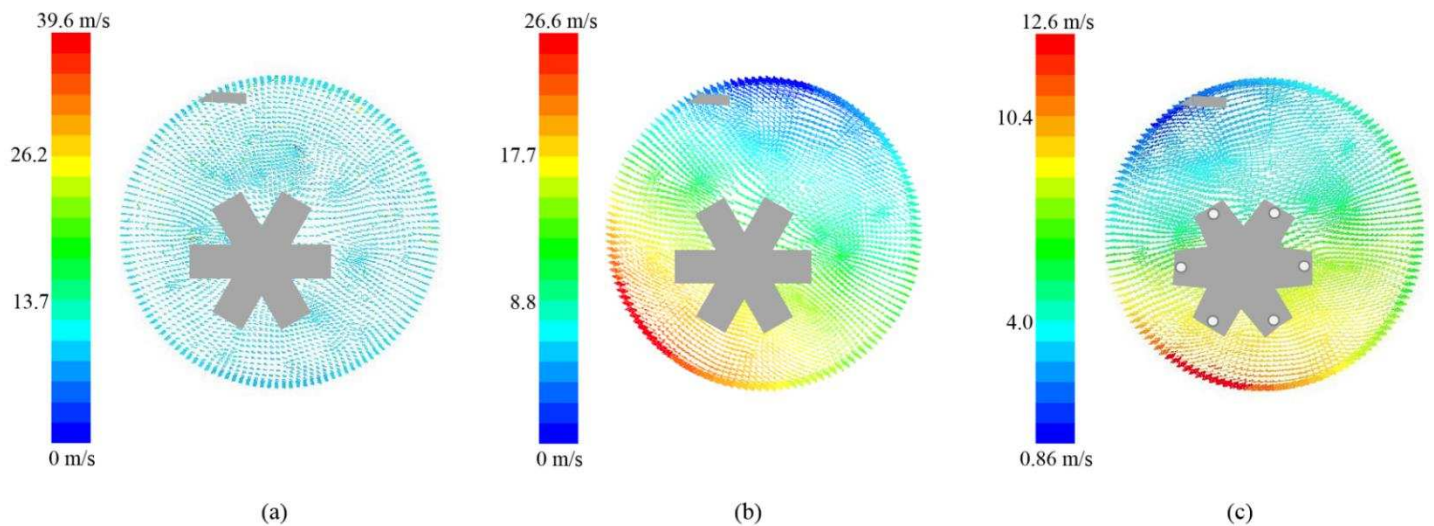


Figure 3. ANSYS based profiles: the velocity profiles of the granules (a) using impeller type II, speed=2000rpm, L/S ratio (w/w)=14%; (b) using impeller type II, speed=6000rpm, L/S ratio (w/w)=15%; (c) using impeller type I, speed=4000rpm, L/S ratio (w/w)=13%.

Figure 3 shows the velocity profiles of the granules for three different experiments. Although the vessel itself was rotating during the experiments, the highest velocities (i.e. radial and tangential velocities) and their gradients can be observed around the impeller area, specifically when the granules are close to both the impeller and the vessel this being due to the values of the tip speed and also to the fact that both of them rotate in the same direction. Such a phenomenon was observed during experiments where the velocity of the impeller is high. It was also observed that the velocity of the granules is still highly dependent on the spatial position of the granules from the impeller, similarly to what was previously reported in¹¹. Thus, different areas have different velocity values, as shown in Figure 3 (b) and (c). However, such a behaviour cannot be observed when the impeller speed is low, which can probably lead to relatively homogeneous mixing features¹¹, as presented in Figure 3 (a). It is worth noting that the velocity scale shown in Figure 3 (a) is wider compared to Figure 3 (b) and (c), however, the granule velocity value in (a) is smaller and it reflects the impeller and the vessel speed value (i.e. tip speed). Under the same operating conditions, the range of the

velocity values for impeller type II model is wider than the one for impeller type I, which may be due to the difference in the geometry and contact area.

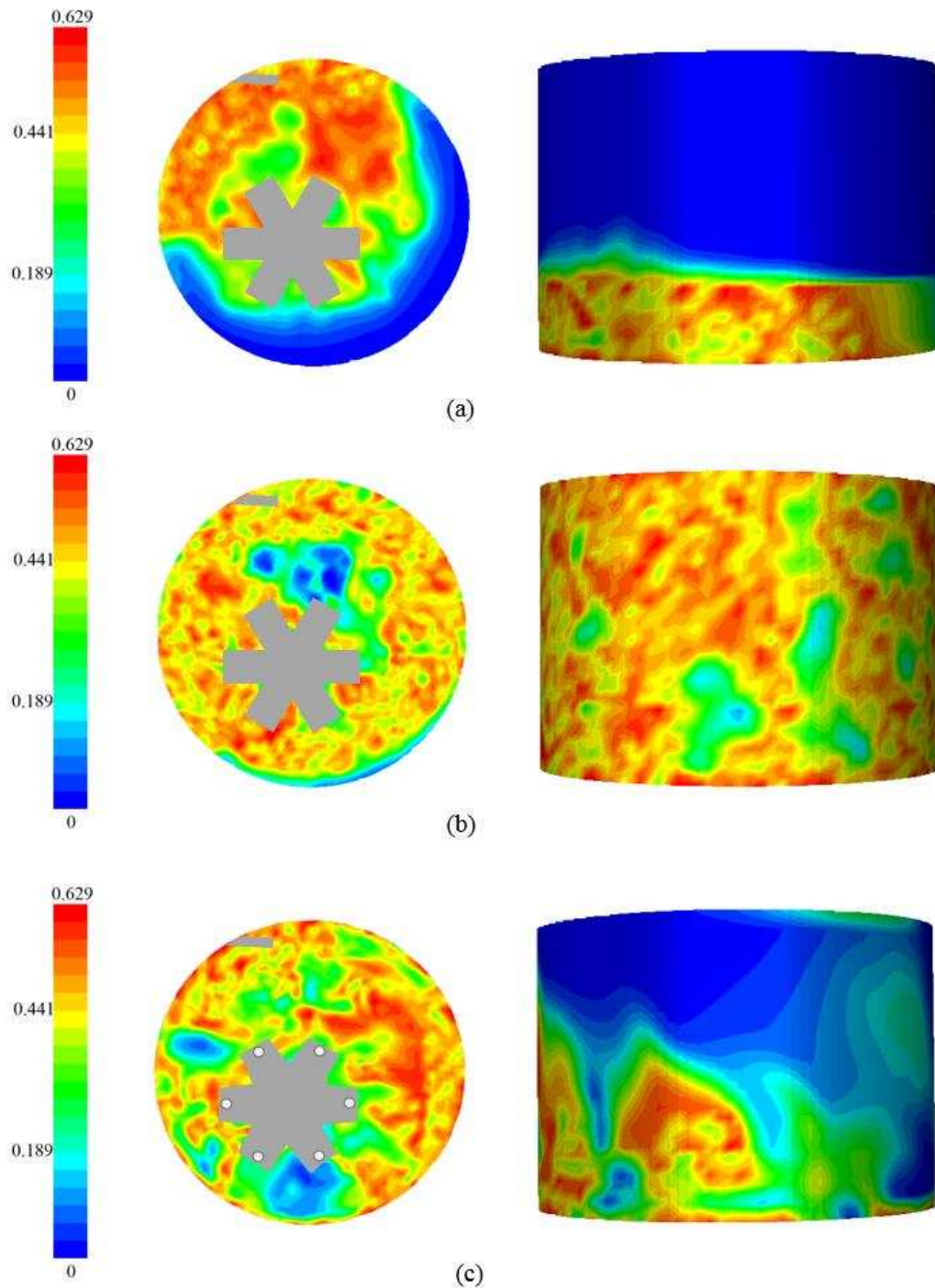


Figure 4. ANSYS based profiles: the concentration of the granules: top (at approximately 3cm from the base) and side view (a) using impeller type II, speed=2000rpm, L/S ratio (w/w)=14%; (b) using impeller type II, speed=6000rpm, L/S ratio (w/w)=15%; (c) using impeller type I, speed=4000rpm, L/S ratio (w/w)=13%.

The concentration of the granules (volume fraction) inside the mixer is shown in Figure 4. The flow regime of the granules shows that the bed surface undulates as the granules are closer to the impeller. A similar behaviour was observed around the scrapper but the bed height is lower. A maximum bed height occurs when the impeller speed is high (at 6000rpm). Spikes in the concentration of the granules were observed during the experiments, which were carried out using impeller type I, as shown in Figure 4 (c). This may be due to the presence of pins on the upper surface of the impeller. As expected, a heterogeneous distribution of the granules is shown in the figure. It is worth noting at this stage that the concentration of the granules is relatively high around the scrapper area in some experiments, which can be explained if one considers the scrapper as a hindrance, especially, at low impeller speed. A low concentration of the granules appears around the impeller; this is the result of the force that is applied by the impeller driving the granules towards the vessel wall. In addition, low concentration of the granules can also be observed in the upper volume of the vessel, where the gas phase dominates. Such a behaviour is noticeable when the impeller speed is relatively low. Moreover, such a low concentration appears around the centre of the vessel in some experiments as a result of the centrifugal force. In fact, this should be in the centre of the vessel, however, the presence of the impeller, which is not in the centre, and the scrapper may have shifted the force effect.

The initial results of the CFD model prove that the velocity and the concentration of the granules and, accordingly, the granulation rates (e.g. growth and breakage) are indeed dependent on the spatial position of the granules themselves, as also previously reported in the literature¹¹. A compartmental model has already been developed for similar cases in the literature. This model can lead to better results if a sufficient number of compartments is used. However, it is considered to be a computationally-taxing model¹¹. Therefore, the average velocity was instead used to evaluate the parameters of PBM in this study. In fact, such an assumption may have a negative effect on the final predictions of the granule properties if the

empirical parameters were not systematically estimated. However, in this work, this did not seem to have a significant effect since the RBF-based model will internally compensate for this.

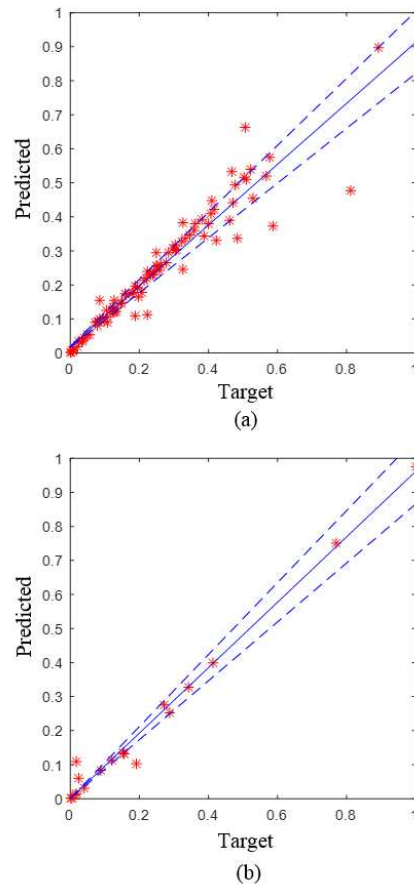


Figure 5. The RBF model for the empirical parameter that is used to estimate the aggregation kernel (normalized): (a) training, (b) testing (with 10% bands) (RBF Network Weights= [1 0.5 0.4 1.5 0.8 1.3 1.3 0.9], and Bias=0.58).

A three-dimensional PBM was also developed, as discussed in ‘The Hybrid Model’ Section. In order to solve the integro-differential equations, a hierarchical algorithm presented in²⁴ was employed in this research paper. This algorithm is based on discretising the three-dimensional population into a number of bins represented as finite volumes. This hierarchical framework enables the user to pre-calculate the time-independent terms of the kernels. As

stated previously, estimating the kernels (e.g. aggregation kernel) depends on empirical parameters. These parameters were evaluated to match the experimental results, followed by mapping the parameters to the granulation input variables by using the RBF model. A single RBF model was developed to learn the relationships among all the input variables (i.e. operating conditions) and the empirical parameters of PBM. For the empirical parameter (ζ) that is used to estimate the size dependent aggregation kernel presented in (3), 8 RBFs, which correspond to the minimum error calculated using the RMSE, were selected. The prediction performance is presented in Figure 5. The RMSE values (training=0.055, testing=0.035) indicate that the model can be used successfully to predict this parameter. Similarly, the model led to a good performance for all the empirical parameters considered.

Using the estimated empirical parameters, the properties of the granules were predicted. Since the granule size has a significant effect on the granule velocity and its distribution, the predicted size was then used to update the parameters of the CFD model. These steps were repeated until the difference between the predictions for two consecutive steps became very small. Figure 6 shows the prediction results for three experiments carried-out under varying operating conditions. In a similar manner, the properties of the granules were predicted for all experiments. The number of iterations for the experiments varied, and generally this numbers was in the range of 6 to 10. The predictive performances for all experiments demonstrate the ability of the hybrid model to predict the properties successfully and to implicitly compensate for the assumptions that have been made about the granulation process. Moreover, the presented model outperformed the three-dimensional PBM. Figure 7 shows an example of the predictive performance of PBM. The PBM performances for the binder content and porosity are not as good as the hybrid model ones, and it is apparent that these performances are worse than the ones for size.

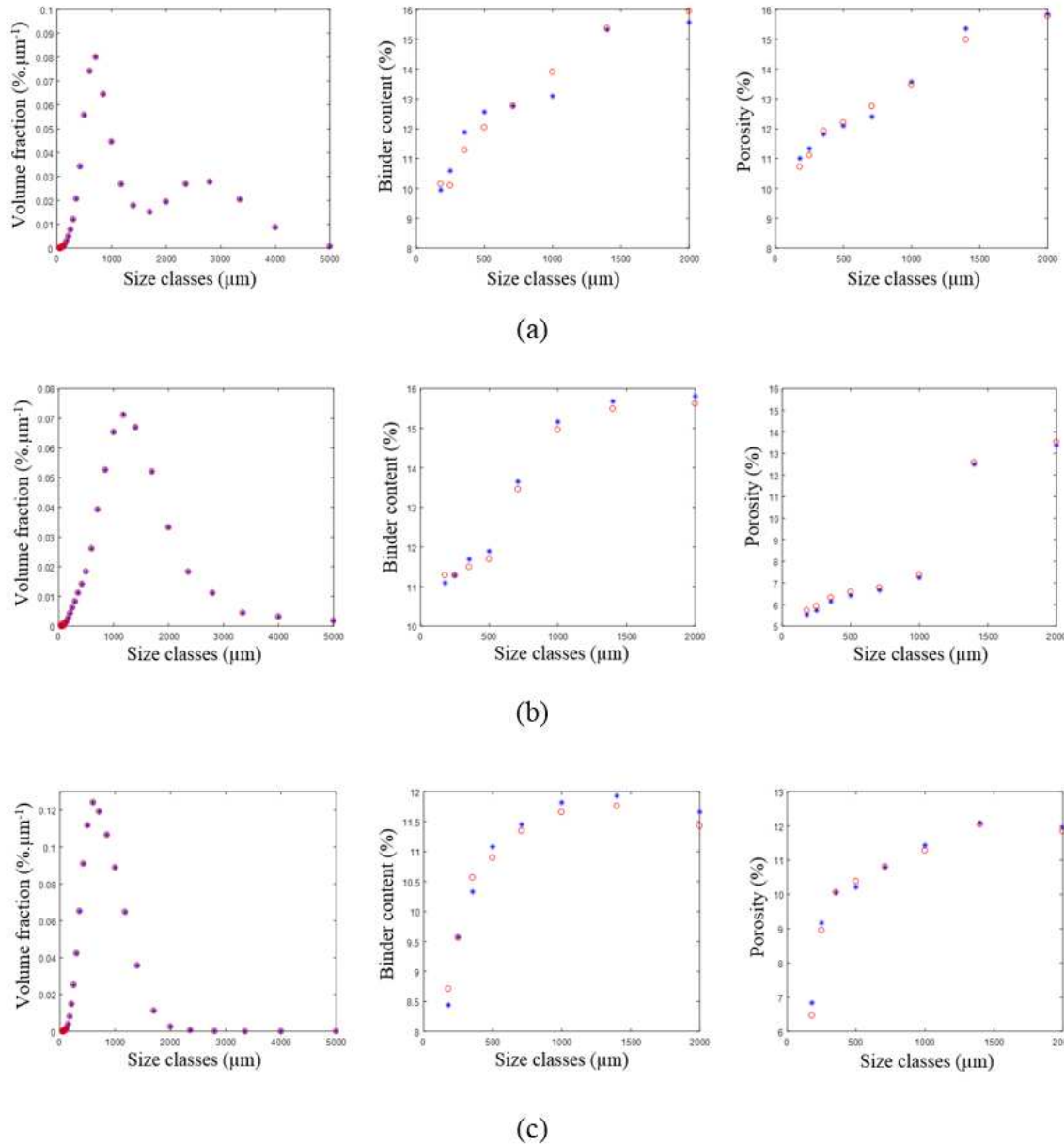


Figure 6. The hybrid model: the predicted (o) and the experimental (*) distributions for the size, binder content and porosity (a) using impeller type II, speed=2000rpm, L/S ratio (w/w)=14% and granulation time=10min; (b) using impeller type II, speed=6000rpm, L/S ratio (w/w)=15% and granulation time=15min; (c) using impeller type I, speed=4000rpm, L/S ratio (w/w)=13% and granulation time=6min.

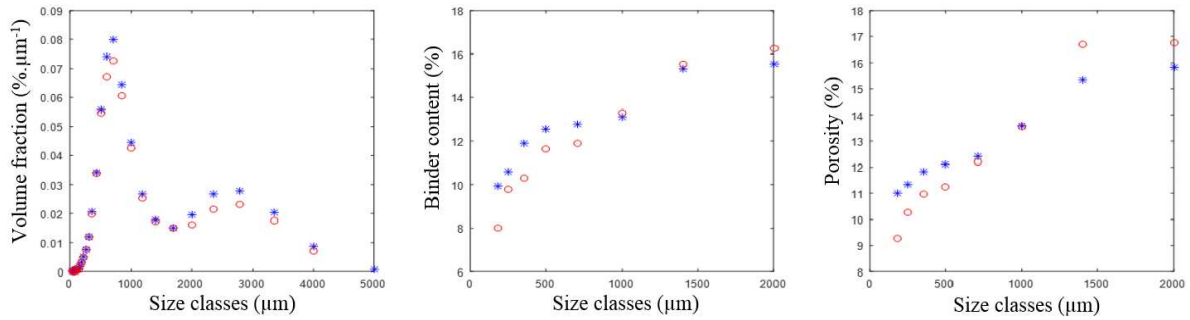


Figure 7. The population balance model: the predicted (○) and the experimental (*) distributions for the size, binder content and porosity using impeller type II, speed=2000rpm, L/S ratio (w/w)=14% and granulation time=10min.

Although, the hybrid model satisfactorily modelled the granulation process, such a model can be further improved. This model initiated the simulation process using the nuclei instead of the particles, this being due to the difficulty of taking account of three phases in the CFD model. Therefore, the hybrid model can be implemented in two stages; the first stage considers the binder and the particles, whereas the second stage considers the granules and gas, followed by integrating the two stages together. Moreover, further investigations will need to be performed to explore the advantages and the limitations of developing such a complex model.

Model Fusion

Model Fusion: The Basic Idea

One of the basic concepts of cognitive process used by human is information fusion. In simple terms, fusion is integrating information from various sources to realise effective inferences and generate optimal decisions²⁵. The motivation for this process lies in the fact that the information provided from one source are, more often than not, limited and with limited accuracy²⁵. Therefore, information fusion has been extensively applied in many areas, including marine technology, manufacturing as well as health care, to ultimately improve the

reliability of information. Various approaches have been developed and used such as Bayesian inference, neuro-fuzzy and the Dempster-Shafer (DS) theory²⁶⁻²⁷. The latter approach has attracted a lot of interest; this being due to its ability to explicitly estimate imprecision and conflict that may exist between two or more sources of information. However, in order to develop a more reliable fusion model, one should consider three types of uncertainties; uncertainty due to probabilities, uncertainty due to lack of specification and uncertainty due to fuzziness²⁸. The first two types can usually be tackled via DS theory, while the third type can be successfully handled using fuzzy logic. Therefore, a new approach that integrates both the DS theory and fuzzy logic has been presented in this research paper. The motivation for such an algorithm stems from the strong need to improve the output predictions of the granulation process which is considered to be one of the complex process to be modelled and predicted. The proposed algorithm integrates the predicted outputs from both the hybrid model and the incorporated model. The fusion model was developed not only to obtain more accurate predictions, which may not be obtainable by using a single model, but also to resolve any conflict that may exist between the two models. Figure 8 summarises the main steps of the proposed fusion model.

First of all, the number of clusters is defined. Generally, clustering is an unsupervised learning process that aims to discover groups of similar data points within the data set. The optimal number of clusters is subjective, in other words, it depends on the application. In this study, the best number of clusters is the one that corresponds to the maximum improvement in the predictive performance (i.e. the minimum RMSE). This step is followed by clustering the input variables and the error residuals that result from both the hybrid model and the incorporated model. The membership function value is defined for each data point as follows²⁹:

$$\mu_i = \exp\left(\frac{-(x_i^e - M)^2}{2 \times \sigma^2}\right) \quad (9)$$

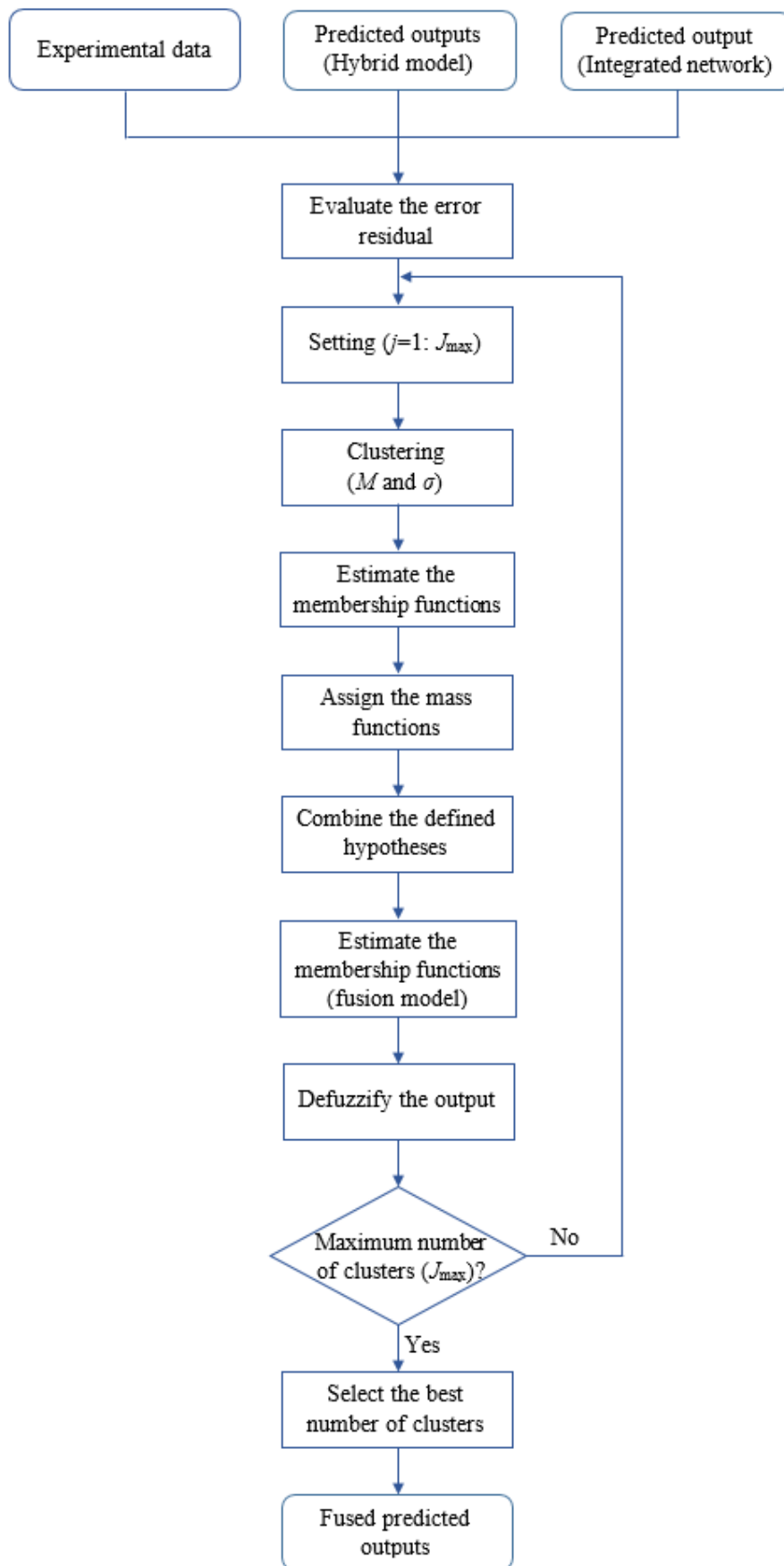


Figure 8. Flow chart of the fusion model.

where μ_i is the membership function of the i^{th} data point. The parameters M and σ represent the mean and the standard deviation of a cluster, respectively, and X_i^e is the residual error.

In order to combine the predicted outputs of the hybrid model with the ones of the incorporated model, the DS theory is utilized. One of the main challenges in implementing the DS theory is assigning the mass function for all the examined hypotheses. In fact, the mass function can be derived using different algorithms such as probabilities or distance from the centre of a cluster³⁰. In this research, the mass function has been evaluated using the fuzzy membership function, which is calculated in (9). The mass function is generally governed by the following set of equations²⁸:

$$m_t = \left(1 - \sum_{\substack{j=1 \\ j \neq t}}^{J_{\max}} \mu_j \times (\eta - \mu_j) \right) \times \mu_t \quad (10)$$

$$\eta = \arg \max_{1 \leq j \leq J_{\max}} \mu_j$$

where m_t is the mass function for the t^{th} hypothesis, and η is the maximum membership function. If the number of clusters is less than or equal to three, then special cases are considered²⁸. The hypotheses are merged using the Dempster's rule of combination as follows:

$$m_{\text{FM}} = \frac{1}{1-K} \sum_{\text{HM} \cap \text{IM} \neq \phi} m_{\text{HM}} m_{\text{IM}} \quad (11)$$

$$K = \sum_{\text{HM} \cap \text{IM} = \phi} m_{\text{HM}} m_{\text{IM}}, \quad K \neq 1$$

where the mass functions for the hypotheses of the fusion, hybrid and incorporated models are distinguished by the subscripts FM, HM and IM, respectively. The parameter K measures the conflict between two sources, and it is also used to estimate the normalization factor, which is equal to $(1-K)$. A hypothesis of the hybrid model is usually combined with the hypotheses of the incorporated model that have the same or better degree of accuracy, and vice versa. To

elucidate, assume that the number of clusters for both models is three (i.e. good, satisfactory and bad), as presented in Figure 9. To estimate the mass function for the ‘satisfactory’ hypothesis of the fusion model, the ‘satisfactory’ hypothesis of the incorporated model should be combined with the ‘good’ and ‘satisfactory’ hypotheses of the hybrid model, and the ‘satisfactory’ hypothesis of the hybrid model should be combined with the ‘good’ one of the incorporated model, note that the combination of the ‘satisfactory’ hypotheses has already been considered. A high degree of conflict between a hypothesis and another less accurate one is assumed, thus, the fusion model can lead to a better performance compared to both the hybrid model and the incorporated model.

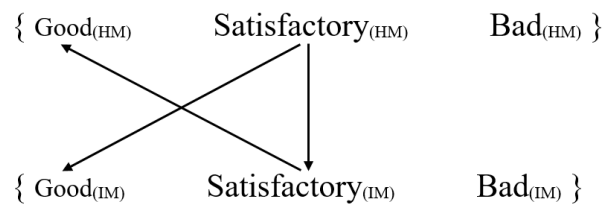


Figure 9. Example of combining the clusters.

Once the mass functions of the fusion model are estimated, the membership functions can be calculated by solving the set of equations in (10), which is reversed to calculate the membership functions, which need to be weighted and normalized²⁸. Finally, the height defuzzifier is utilized to evaluate the outputs of the fusion model²⁹.

Model Fusion: Results and Discussions

The algorithm relating to the fused model was implemented to improve the performance of the two models; the hybrid model and the incorporated model, especially, in those areas where the performance of one of the models or both was not as close to the target as desired. Thus, the granulation input variables and the error residuals have been used to identify these

areas. For instance, Figure 10 shows how the hybrid model performs in one of the space areas (i.e. clusters) of the binder content. Such a figure indicates that the hybrid model performance measured via the error residuals is satisfactory when the impeller is of type I, the impeller speed is medium, the granulation time is small and the L/S ratio is medium. It is worth mentioning that the impeller shape was considered as a crisp variable instead of a singleton, as shown in Figure 10.

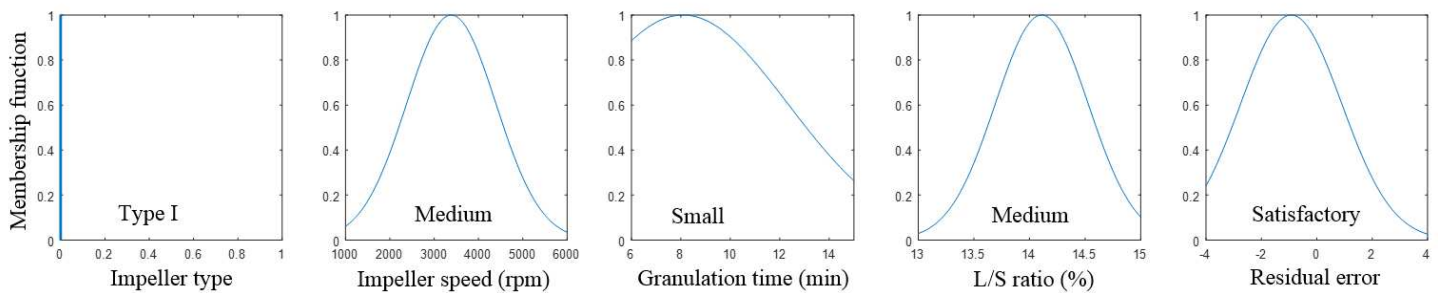
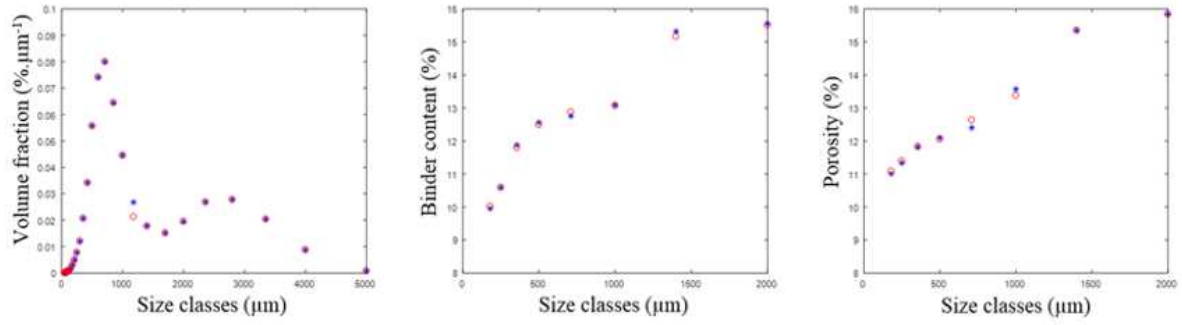
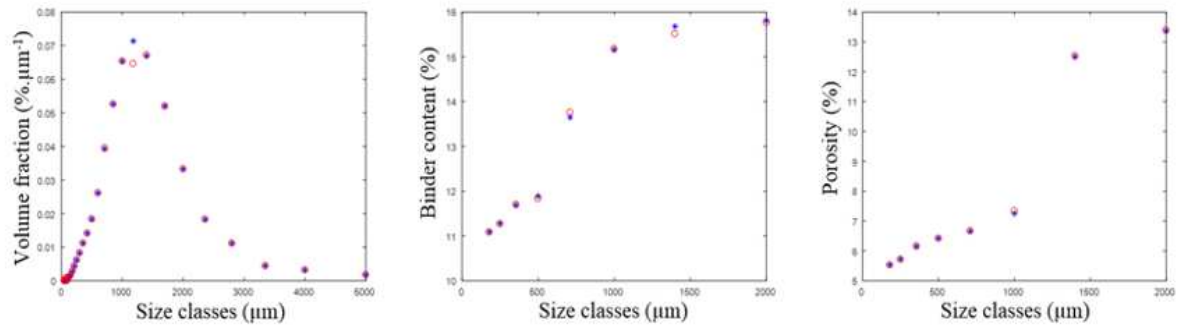


Figure 10. An example of the hybrid model performance in the space area of the binder content.

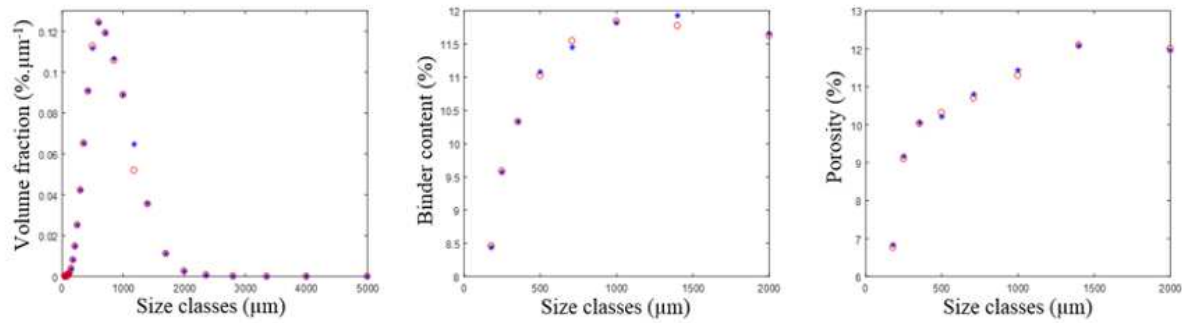
As summarised in Figure 8, the estimated membership functions were used to assign the mass functions for the hypotheses of both models. Next, the mass functions were combined using the set of equations in (11). This led to the mass functions for the hypotheses of the fusion model. To estimate the membership functions of the fusion model clusters, the set of equations in (10) were solved numerically, since the analytical solution (i.e. closed form solution) may be computationally taxing, in particular, when the number of clusters is large. After the defuzzification step, the outputs from the fusion model for three experiments are shown in Figure 11, where different numbers of clusters were assigned to the various size classes, these numbers laying in the range of 5 to 9.



(a)



(b)



(c)

Figure 11. The fusion model: the predicted (o) and the experimental (*) distributions for the size, binder content and porosity (a) using impeller type II, speed=2000rpm, L/S ratio (w/w)=14% and granulation time=10min; (b) using impeller type II, speed=6000rpm, L/S ratio (w/w)=15% and granulation time=15min; (c) using impeller type I, speed=4000rpm, L/S ratio (w/w)=13% and granulation time=6min.

The predictive performance of the fused model for all experiments is similar to the one presented in Figure 11, which shows a good performance. In the size class (1180 μ m), the predictive performance is not as good as for the other size classes, because the performance of the incorporated model was slightly lower for this size class. However, the overall improvement is noticeable. Table 1 includes the average coefficients of determination (R^2) and the RMSE performance values of the RBF model (standalone model), which was used here to predict the properties of the granules, PBM (standalone model), the previous model presented in¹, referred to in the table as ‘the incorporated model’, the hybrid model presented in ‘The Hybrid model’ Section, and the fusion model described in ‘Model Fusion’ Section. As shown in this table, the fusion model outperformed both the incorporated and the hybrid models. Furthermore, this table shows that the predictive performance for the size was better than that for the binder content and porosity. This may be due to the heterogeneity and the high uncertainties in the measurements of these properties. However, most of the predictions from the incorporated, hybrid and fusion models lay within the 95% confidence interval.

Table 1. The performances of the models represented by R^2 and RMSE.

Model	RBF ¹		PBM ²		Incorporated Model ³		Hybrid Model ⁴		Fusion Model ⁵	
	R^2	RMSE	R^2	RMSE	R^2	RMSE	R^2	RMSE	R^2	RMSE
Size	53.65	0.0098	75.84	0.0076	87.83	0.0055	88.49	0.0017	91.28	0.0008
Binder Content	46.8	1.2792	67.53	1.0252	74.04	0.9352	76.06	0.6316	80.30	0.5577
Porosity	36.99	1.6457	65.49	1.23	74.02	1.0879	75.67	0.9208	79.54	0.5508

1. The RBF standalone model was utilized to predict the granule properties.
2. The PBM was used as a stand-alone model.
3. The incorporated model includes the integrated network and the Gaussian mixture model as presented in¹.
4. The hybrid model as presented in ‘The Hybrid Model’ Section.
5. The fusion model as described in ‘Model Fusion’ Section.

Assessing the generalization capabilities of the developed models is an important step to prove their effectiveness and efficiency. Thus, the hybrid model has been utilized to predict the properties of the granules produced using different operating conditions but within the investigated ranges. Figure 12 (a) shows the predicted outputs for a new experiment. The predictive performance values for the three properties are comparable to the ones that obtained

using the training data. Similarly, the fused model has been validated using the operating conditions of the new experiment and the predictions from both the hybrid and the incorporated models. The predicted outputs obtained by the fused model are presented in Figure 12 (b). The predictive performance and the generalization capabilities prove the abilities of the hybrid and the fusion models to be used successfully to understand the granulation process and to accurately predict the properties of the granules produced by the HSG process.

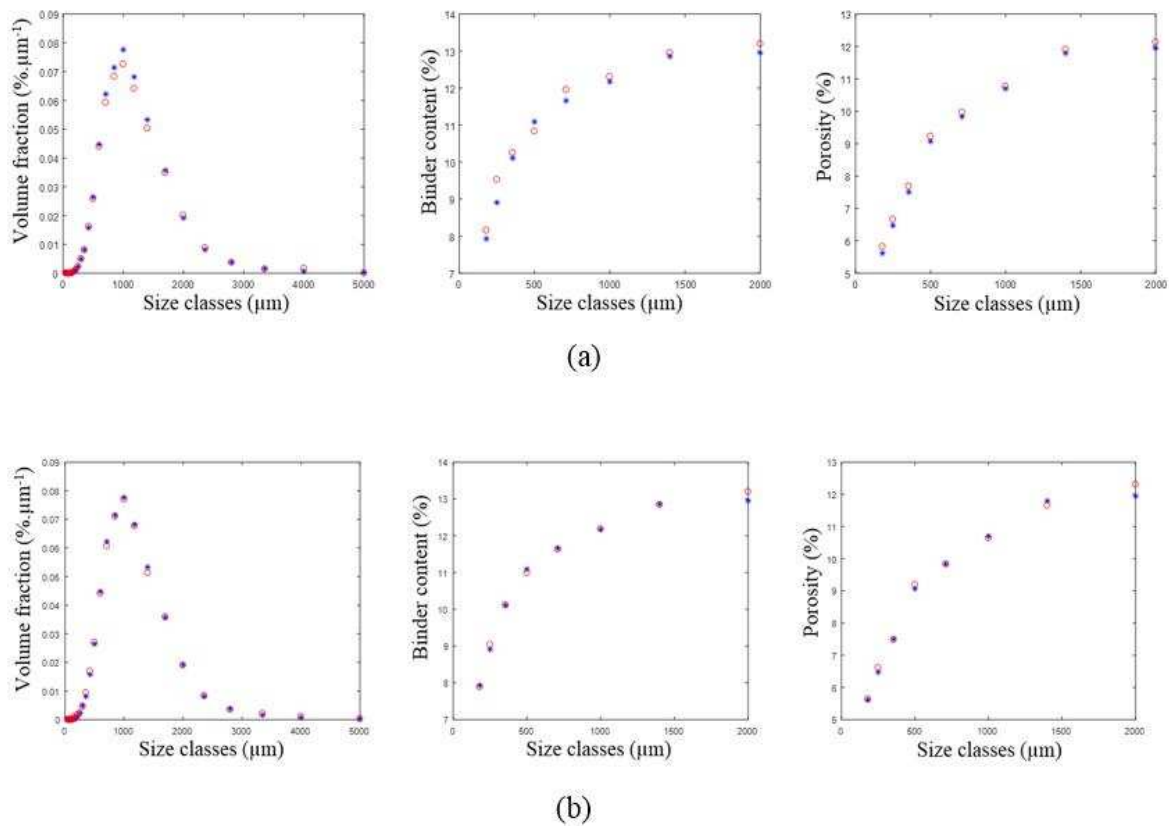


Figure 12. The validation experiment: the predicted (o) and the experimental (*) distributions for the size, binder content and porosity using impeller type I, speed=4400rpm, L/S ratio (w/w)=13.6% and granulation time=12min (a) the hybrid model and (b) the fusion model.

The proposed modelling framework, i.e. the hybrid model followed by the fusion model architecture, successfully modelled the granulation process. This has been achieved by providing good predictions for the properties of the granules and an understanding of the

process and its mechanisms. Generally, one develops models either to predict properties/behaviours or to control a process. The former, which is the main aim of this research, paves the way for the latter. In the future, the developed framework will be exploited in a reverse-engineering framework to identify the optimal operating conditions for granules with predefined properties. This can be achieved by, for instance, embedding the multi-objective optimization paradigms to ensure the right-first-time production.

Conclusions

In this research, a hybrid model based on both physical and data-based models was presented to model the high shear granulation process. The model consisted of three components, namely, a computational fluid dynamics (CFD) model, a population balance model (PBM) and a radial basis function (RBF) model. These models were integrated through an iterative procedure, where the outputs from one of these models are used as inputs to the model architecture. The hybrid model combined the strengths of the single models involved in a way that any potential limitations may be circumvented. Consequently, this model was able to provide a deeper insight into the granulation process and its mechanisms, and also the flow of the granules. It was also capable of interpreting the relationships between the inputs and the outputs, hence it can be used to predict the properties of the granules with a good degree of accuracy. In addition, the model was able to implicitly compensate for some of the basic assumptions normally used in physical models, which were previously reported in the literature. Furthermore, the new model expressed the empirical parameters as a function of the granulation input variables. Although, the RBF model cannot physically interpret the relationship between the inputs and the outputs, these parameters can easily be predicted if one knows the operating conditions of the experiment. The effectiveness and efficiency of the hybrid model was demonstrated and validated by predicting the properties for the training

experimental data and subsequently newly acquired data successfully. By utilizing the scaling-up methods presented in the related literature³¹ and by training the RBF network, the hybrid model can be exploited on a relatively larger scale. However, many aspects need to be considered (e.g. mixer geometry) to ensure that it will be implemented correctly.

Accurate predictions of the properties of the granules are more often than not required. Accordingly, a new fusion model based on integrating fuzzy logic theory and Dempster-Shafer theory was developed. This model combined the predicted outputs from the hybrid model with the corresponding ones from the model incorporating the integrated network and the Gaussian mixture model; such a model is a data-based model that had been developed previously¹. The main motivation behind such a model was, in addition to accurate predictions, to resolve any conflict(s) that may exist between the various model formalisms. Significant improvements were achieved by using this new approach over the hybrid and the incorporated models.

In summary, a good modelling performance was achieved by the hybrid model, followed by the fusion model. Such a framework is considered to be a promising development in those industries where the granulation process is considered to be one of the most crucial unit operations that determine the quality of the final product. In the future, such a framework can be exploited within a reverse-engineering framework that can achieve right-first time production of granules.

Acknowledgement

The Authors wish to thank Maschinenfabrik Gustav Eirich GmbH & Co KG (Germany) for providing the Eirich mixer that has been used for all the experimental work.

References

1. AlAlaween WH, Mahfouf M, Salman AD. Predictive Modelling of the Granulation Process Using a Systems-Engineering Approach. *Powder Technology*.2016; 302:265-274.
2. Benali M, Gerbaud V, Hemati M. Effect of operating conditions and physico-chemical properties on the wet granulation kinetics in high shear mixer. *Powder Technology*.2009; 190:160-169.
3. Litster J. *The science and engineering of granulation processes*. Dordrecht Springer, 2004.
4. Walker G. Future development in drum granulation modelling, In: Salman A, Hounslow M, Seville J (Eds.). *Granulation*. Oxford: Elsevier, 2007:249-254.
5. Bjorn I, Jansson A, Karlsson M, Folestad S, Rasmuson A. Empirical to mechanistic modelling in high shear granulation. *Chemical Engineering Science*.2005;60:3795-3803.
6. Sanders C, Willemse A, Salman A, Hounslow M. Development of a predictive agglomeration model. *Powder Technology*.2003;138:18-24.
7. Braumann A, Goodson M, Kraft M, Mort P. Modelling and validation of granulation with heterogeneous binder dispersion and chemical reaction. *Chemical Engineering Science*.2007;62:4717-4728.
8. Miyamoto Y, Ogawa S, Miyajima M, Matsui M, Sato H, Takayama K, Nagai T. An application of the computer optimization technique to wet granulation process involving explosive growth of particles. *International Journal of Pharmaceutics*.1997;149:25-36.
9. Iveson S. Limitations of one-dimensional population balance models of wet granulation processes. *Powder Technology*.2002;124:219-229.
10. Poon JM, Immanuel CD, Doyle III FJ, Litster JD. A three-dimensional population balance model of granulation with a mechanistic representation of the nucleation and aggregation phenomena. *Chemical Engineering Science*.2008;63:1315-1329.
11. Yu X, Hounslow MJ, Reynolds GK, Rasmuson A, Bjorn IN, Abrahamsson PJ. A compartmental CFD-PBM model of high shear wet granulation. *AIChE Journal*.2016.

12. Sen M, Barrasso D, Singh R, Ramachandran R. A multi-scale hybrid CFD-DEM-PBM description of a fluid-bed granulation process. *Processes*.2014;2:89-111.
13. Dareluisa A, Remmelgasc J, Rasmusona A, Wachemb B, Bjorn IN. Fluid dynamics simulation of the high shear mixing process. *Chemical Engineering Journal*.2010;164:418-424.
14. Ramkrishna D. Population balances: theory and applications to particulate systems in engineering. London: San Diego Calif., 2000.
15. Liu L, Zhou L, Robinson D, Addai-Mensah J. A nuclei size distribution model including nuclei breakage. *Chemical Engineering Science*.2013;86:19-24.
16. Immanuel CD, Doyle III FJ. Mechanistic modelling of aggregation phenomena in population balances of granulation processes. *IFAC Proceedings Volumes*.2005;416-421.
17. Pinto MA, Immanuel CD, Doyle III FJ. A feasible solution technique for higher-dimensional population balance models. *Computers and Chemical Engineering*.2007;31:1242-1256.
18. Nguyen D, Rasmuson A, Bjorn IN, Thalberg K. CFD simulation of transient particle mixing in a high shear mixer. *Powder Technology*.2014;258:324-330.
19. Dareluis A, Rasmuson A, Wachem B, Bjorn IN, Folestad S. CFD simulation of the high shear mixing process using kinetic theory of granular flow and frictional stress models. *Chemical Engineering Science*.2008;63:2188-2197.
20. Wen CY, Yu YH. Mechanics of fluidization. *Chemical Engineering and Processing: Process Intensification*.1966;62:100-111.
21. Gidaspow D. *Multiphase Flow and Fluidization: Continuum and Kinetic Theory Descriptions*. London: Academic Press, 1994.
22. Tu JY, Fletcher CAJ. Numerical computation of turbulent gas–solid Particle Flow in a 90° bend. *AIChE Journal*. 1995;41:2187-2197.
23. Bishop C. *Neural Networks for Pattern Recognition*. New York:Clarendon Press, 1995.

24. Immanuel CD, Doyle III FJ. Solution technique for a multi-dimensional population balance model describing granulation processes. *Powder Technology*.2005;156:213-225.
25. Frikha A, Moalla H. Analytic hierarchy process for multi-sensor data fusion based on belief function theory. *European Journal of Operational Research*.2015;241:133-147.
26. Dempster AP. Upper and lower probabilities induced by a multivalued mapping. *The Annals of Mathematical Statistics*.1967;38:325-339.
27. Maselena A, Hasan MM, Tuah N, Tabbu CR. Fuzzy logic and mathematical theory of evidence to detect the risk of disease spreading of highly pathogenic avian influenza H5N1. *Procedia Computer Science*.2015;57:348-357.
28. Boudraa A, Bentabet A, Salzenstein F, Guillon L. Dempster-Shafer's basic probability assignment based on fuzzy membership functions. *Electronic Letters on Computer Vision and Image Analysis*.2004;4:1-9.
29. Mendel JM. Uncertain rule-based fuzzy logic systems: introduction and new directions. Prentice Hall, 2001.
30. Bloch I. Some aspect of Dempster-Shafer evidence theory for classification of multimodality medical images taking partial volume effect into account. *Pattern Recognition Letters*.1996;17:905-916.
31. Watano S, Okamoto T, Sato Y, Osako Y. Scale-up of high shear granulation based on the internal stress measurement. *Chemical & Pharmaceutical Bulletin*.2005;53:351.